Journal Pre-proofs

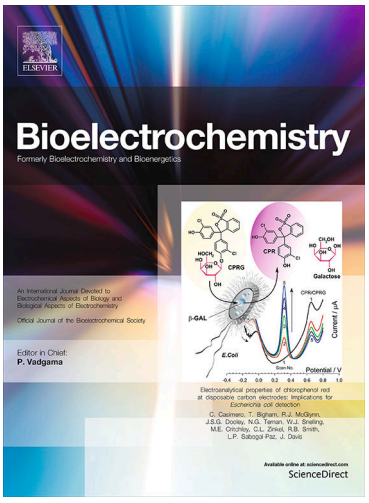

Ultrasensitive detection of interleukin 1α using 3-phosphonopropionic acid modified FTO surface as an effective platform for disposable biosensor fabrication

Elif Burcu Aydın, Mustafa Kemal Sezgintürk

PII: S1567-5394(20)30621-6
DOI: https://doi.org/10.1016/j.bioelechem.2020.107698
Reference: BIOJEC 107698

To appear in: *Bioelectrochemistry*

Received Date: 25 August 2020
Revised Date: 21 October 2020
Accepted Date: 31 October 2020

Please cite this article as: E. Burcu Aydın, M. Kemal Sezgintürk, Ultrasensitive detection of interleukin 1α using 3-phosphonopropionic acid modified FTO surface as an effective platform for disposable biosensor fabrication, *Bioelectrochemistry* (2020), doi: https://doi.org/10.1016/j.bioelechem.2020.107698

Ultrasensitive detection of interleukin 1α using 3-phosphonopropionic acid modified FTO surface as an effective platform for disposable biosensor fabrication

Elif Burcu Aydın[a*], Mustafa Kemal Sezgintürk[b]

[a]Tekirdağ Namık Kemal University, Scientific and Technological Research Center, Tekirdağ-Turkey

[b]Çanakkale Onsekiz Mart University, Faculty of Engineering, Bioengineering Department, Çanakkale, Turkey

***Corresponding Author:**

e-mail: b_e_bahadir@hotmail.com

ebbahadir@nku.edu.tr

Tel:+90 282 250 11 37

Abstract

In this study, we utilized a carboxyalkylphosphonic acid covered fluorine doped tin oxide (FTO) as an electrode material for fabrication of Interleukin 1α (IL-1α) immunosensor. For this aim, anti-IL-1α antibodies were attached on the 3-phosphonopropionic acid (PHP) modified FTO surface covalently. Electrochemical (electrochemical impedance spectroscopy and cyclic voltammetry) and morphological (scanning electron microscopy and atomic force microscopy) characterizations were performed to monitor the successful fabrication of immunoelectrodes. After incubation of anti-IL-1α antibody immobilized FTO electrodes in IL-1α antigen solutions, increases were seen in impedimetric responses. IL-1α antigen was determined in a linear detection range from 0.02 to 2 pg/mL by EIS. The detection limit of the suggested immunosensor was 6 fg/mL. The applicability of the designed biosensor was tested by using human serum and saliva samples and acceptable results were obtained. In addition, high sensitivity, good specificity, low detection limit made the proposed immunosensor a potential technique for IL-1α antigen determination in routine clinical analysis.

Keywords: 3-phosphonopropionic acid, interleukin-1α, fluorine doped tin oxide, impedimetric biosensor.

1. Introduction

Cancer is a complex and harmful disease and it affects the human health in worldwide with a high rate of mortality. According to latest cancer statistics, the growth rate of cancer cases will increase in next few years due to some factors such as work, diet and environment. Biomarkers are medical signs and indicate the health status of patients. The accurate detection of tumor biomarkers provides essential information about disease conditions. Therefore, the new method development is necessary to detect tumor biomarkers accurately and quickly in human fluids for early cancer diagnosis and treatment. Saliva is an important biofluid and contains water (about 99%), electrolytes (sodium, potassium, calcium, chloride, magnesium, bicarbonate, phosphate), glucose, enzymes, immunoglobulins, glycoproteins, and polypeptides. These components are important for human health and therefore, saliva is a possible diagnostic tool for disease diagnosis and treatment monitoring. Saliva collection provides several advantages over blood, such as being easy, simple and non-invasive. The biomarker level in saliva is very low. Therefore, the development of sensitive techniques and biosensing methods is important for disease diagnosis and monitoring. There are several commercially available protein assay tools, but these tools are suitable for laboratory testing and non-suitable for point-of-care applications. In addition, these tools are currently used for detection of glucose, different hormones, bacteria [1-4].

Interleukin 1 is a multifunctional cytokine and has a role in development of inflammatory and immunological responses [5]. IL 1 gene family on chromosome 2q14.2 includes the three related genes (IL-1α, IL 1β and IL-RN), which encode IL-1α, IL 1β and their endogenous receptor antagonist (IL-IRA), respectively [6]. These cytokines are produced in several cell types such as monocytes, macrophages and epithelial cells [7]. IL-1α is a membrane-anchored molecule and has an autocrine signaling mechanism [8]. Furthermore, IL-1α increases the permeability of the endothelial cell monolayers [9]. The role of IL 1α in carcinogenesis has been investigated extensively. Experimental results illustrate the vital role of IL-1α in breast [6], oral squamous cell [10, 11], head and neck squamous cell [12, 13] and tongue cancer [14]. The levels of IL-1α antigen in oral squamous cell cancer patient were 0-137 pg/mL and 175-1000 pg/mL in human serum and saliva, respectively [15].

As mentioned above, IL-1α is a very important biomarker in the biological and pathological events. Therefore, enzyme-linked immunosorbent assay (ELISA) kits and biosensors for specific detection of IL-1α have been developed. There are not many biosensors developed in the literature for the quantification of IL-lα. Because of this, this developed immunosensor is vital for the quantification of IL-1α level in biological fluids. Tao et al. (2006) developed protein imprinted xerogels with integrated emission sites (PIXIES) without utilizing biorecognition molecule for IL-1α detection. To fabricate the PIXIES sol–gel derived xerogels, molecular imprinting, and a luminescent reporter element were used. Interaction between the template site and IL-1α changed the physicochemical properties which were detected with a luminescent probe molecule [16]. An optical biosensor was developed for the investigation of binding kinetics between interleukin 1 receptor and IL-1α. IL-1α was attached on the carboxymethyl dextran surface via amide bonds formed between amino groups of IL-1α antigen and

carboxyl groups of carboxymethyl dextran. The linear range and detection limit of this optic biosensor was 100-1600 nM and 100 nM, respectively [17]. A quantum dot (QD) based electrochemical immunoassay was fabricated for IL-1α detection. QD conjugated anti-IL-1α antibody was utilized as a label in biorecognition event and the principle of this immunoassay based on a sandwich immunoreaction. Electrochemical voltammetric stripping analysis was employed to determine the level of IL-1α antigen. The linear range and detection limit were found as 0.5-50 ng/mL and 0.3 ng/mL, respectively. The developed immunoassay gave reproducible results and it was suitable for biomarker detections [18].

Transparent conductive oxides (TCO) are semi-conductive materials and have been extensively utilized in recent years in different fields such as solar cells, electrochemistry, display applications, electrochromic mirrors [19]. They have a special role in electrochemistry, and they are utilized as transparent electrodes for optoelectrochemical and electrochemical experiments [20]. Fluorine-doped tin oxide (F-doped SnO_2, FTO) glass is one of the commercially available conductive oxide (TCO) substrates and it has great potential to replace the currently most popular TCO, tin-doped indium oxide (ITO). ITO is more expensive than FTO owing to the scarcity of indium on Earth. Moreover, FTO is more stable than ITO in thermal conditions. It has high optical transparency in the visible range of spectrum and good electrical conductivity. FTO has many applications as transparent conducting electrode in flat panel displays, LCD's, electro chromic instruments, organic light emitting diodes and transparent conductive transistors. In recent years, FTO has been used in solar cells, optoelectronic devices, thiols oxidation, lipoic acid quantification, photoelectrochemical biosensors and hydrogen peroxide biosensing [21-22]. Additionally, FTO provides direct observations of electrode morphology, with confocal microscopes before and after attachment of biorecognition element and desired analyte [23]. In recent years, gold, glassy carbon electrode and indium tin oxide have been used as working electrodes in different applications. However, these working electrodes are more expensive than FTO electrodes. Therefore, we select FTO glass as a working electrode for development of IL-1α biosensor. FTO-glass substrates show high electrical conductivity, high chemical and mechanical stability, good transparency. In addition, they eliminate the problem of diffusion as seen in case of ITO sheets [24].

A critical stage while fabrication of an immunosensor is the immobilization of antibodies on the electrode. The amount of immobilized antibody will affect the accuracy, sensitivity and stability of an immunosensor. Several modification routes have been developed for electrode surface preparation [25, 26]. Electrodeposition [27-29], electropolymerization [30, 31], anodic treatment [23] techniques have been utilized for FTO biosensor construction. The unique properties of the phosphonates to form a self-assembled monolayer (SAM) on different metal oxides like Al_2O_3, SiO_2, Fe_2O_3, Fe_3O_4, In_2O_3, SnO_2, ITO etc., provide a modified platform for biorecognition elements such as enzymes, antibodies, aptamers immobilization [32, 33]. Silanes, carboxylic acids, and phosphonic acids have been utilized to construct the SAMs on metal oxides. Generally, silanes are usually utilized to form multilayers on metal oxide surfaces. Carboxylate SAMs on metal oxide surfaces are not stable because they rely on the

electrostatic interactions between the adsorbate and the surface. However, phosphonic acids form monolayers on metal oxide surfaces in either aqueous or organic solutions, and the phosphonate SAMs are more stable than either silane or carboxylate SAMs. Therefore, phosphonate SAMs become more popular than silane and carboxylate SAMs due to their good stability [34]. In addition, phosphonic acid binds more strongly than carboxylic acids to metal oxides by forming well-packed SAMs [35]. Compared to some types of silane SAMs, the phosphonate SAMs have a better surface coverage and hydrolytic stability. The phosphonate SAMs are more stable than thiol SAMs on gold under ambient conditions for a greater time due to higher bond energy (P-O bond energy: 80 kcal/mol; S-Au bond energy: 40 kcal/mol). These features make phosphonate SAMs very promising platforms for different applications [36].

The aim of the present work was to fabricate a new electrochemical immunosensor for IL-1α biomarker detection. The proposed immunosensor had a simple fabrication protocol without need to use any high-cost matrix material. PHP, a carboxyalkylphosphonic acid, was used as matrix material for immobilization of IL-1α antibodies, which were the biorecognition elements of IL-1α antigens. PHP formed a stable SAMs on the FTO electrode and it was used as an immobilization matrix to prepare a sensitive immunosensor for the first time. PHP was not only a good biorecognition element immobilization matrix material for the fabrication of biosensor, but also it was a low-cost interface material and reduced the cost of the immunosensor. Additionally, this study illustrated the applicability of phosphonic acid-based surface on biosensing technology. Moreover, FTO electrode was cheaper than traditional electrodes such as gold, platinum, glassy carbon electrode and screen-printed electrode. FTO electrode had good electrical conductivity and high stability. Because of these promising properties of FTO electrode, it was chosen as an immobilization platform. In order to quantify the IL-1α antigen, EIS technique was utilized as an analytical technique. The variations formed on the FTO electrode surface were followed by EIS and cyclic voltammetry (CV) measurements. During the electrochemical analyses potassium ferricyanide/ferrocyanide ($[Fe(CN)_6]^{3-}/[Fe(CN)_6]^{4-}$) was employed as an electrochemical redox couple. After immobilization of IL-1α antigen on the FTO surface, an increase was measured in impedance response because of the immunocomplex formation between anti-IL-1α antibody and IL-1α antigen. The suggested biosensor had high sensitivity, excellent selectivity, excellent repeatability and reproducibility, and acceptable recovery. Its high sensitivity was originated from specific interaction between immobilized anti-IL-1α antibody and IL-1α antigen.

2. Experimental

2.1 Chemicals and Reagents

Acetone, soap solution, hydrogen peroxide (H_2O_2), ammonium hydroxide (NH_4OH), 3-phosphonopropionic acid, $K_3[Fe(CN)_6]$, $K_4[Fe(CN)_6]$, dimethyl sulfoxide (DMSO), N-[3-(dimethylaminopropyl)-N-3-ethylcarbodiimide hydrochloride] (EDC), N-hydroxysuccinimide (NHS), potassium chloride, potassium monohydrogen phosphate, potassium di-hydrogen phosphate, anti-IL-1α antibody (goat), IL-1α antigen (human), tumor necrosis factor α (TNF α), interleukin 8 (IL 8), interleukin

6 (IL 6), interleukin 1β (IL-1β) and bovine serum albumin (BSA) were from Sigma-Aldrich. FTO coated glass (200 mm x 100 mm x 2.3 mm, resistance 10 U sq^{-1}) was purchased from Teknoma Technological Materials Industrial and Trading Inc. Antibody, antigen, and BSA solutions were prepared by using phosphate buffer (pH 7.4, 50 mM) and stored -20 ^{o}C until use. All analyses were performed at room temperature.

2.2. Instrumentation

Electrochemical analyses were performed on a Gamry Potentiostat/Galvanostat (Reference 1000) Instruments containing a conventional three-electrode cell system (Ag/AgCl reference electrode, a platinum wire counter electrode and FTO glass working electrode). Scanning electron microscopy (SEM) images of the fabrication steps were taken by FEI-Quanta FEG 250 scanning electron microscope and, Atomic force microscopy (AFM) images of the fabrication steps were recorded by NanoMagnetic Instruments, AFM PLUS+ in the tapping mode using standard Si_3N_4 cantilevers. Fourier Transform Infrared (FTIR) analyses were carried out utilizing a Bruker Company Vertex 70 FTIR infrared spectrometer in the range of 4000–400 cm^{-1} at room temperature and the results were used without any corrections. Dispersive Raman measurements were carried out with a Thermo company DXR Raman spectrometer equipped with a 780-nm excitation laser and a confocal microscope with 3 objectives.

2.3 Fabrication of modified FTO electrodes

Firstly, FTO substrate was cleaned with acetone, soap solution and ultrapure water in ultrasonic bath successively. Then, FTO electrode was treated with H_2O/H_2O_2 (30%)/NH_4OH (25%) solution (5:1:1 vol) at room temperature for 90 min to form hydroxyl groups on FTO surface, followed by thorough rinsing with ultrapure water to form an impurity-free surface. PHP (0.05 mM) was prepared in DMSO-ultrapure water (1:1) solution. After that, FTO substrate was immersed in PHP solution overnight to form a PHP layer on the FTO substrate and washed with ultrapure water. Thus, carboxyl groups were introduced on the FTO substrate surface. In order to activate the carboxyl groups on the FTO substrate, FTO substrate was immersed in NHS (0.1 mM) / EDC (0.4 mM) solution for 1h. Afterward, the FTO surface was rinsed with ultrapure water and dipped in phosphate buffer solution containing IL-1α antibodies. The anti-IL-1α immobilized FTO electrode was washed with ultrapure water to eliminate any unbound molecules. Covalent bonds formed between the NHS/EDC activated -COOH groups of PHP and amino groups of antibodies. The free carboxyl ends were blocked by BSA. After blockage with BSA solution, the FTO electrodes were rinsed with ultrapure water to eliminate any unbound BSA molecules. The further binding of IL-1α antigen on the IL-1α antibodies immobilized FTO substrate illustrated strong specific antibody-antigen interaction.

2.4 Preparation of saliva and serum samples

Human saliva samples were collected from volunteers after rinsing the mouth thoroughly with water. Before the analysis of saliva samples, they were centrifuged for 10 min at 3000 rpm and then, they were diluted 200-fold with phosphate buffer (pH 7.4 50 mM). The serum samples were obtained from

Tekirdağ Namık Kemal University, Faculty of Medicine with research ethics committee approval and they were diluted 20-fold with phosphate buffer (pH 7.4 50 mM) before the analysis. The determination of IL-1α was performed by applying the procedure described above using a 100 µL of the diluted sample.

2.5 Electrochemical Measurements

The modified FTO substrates fabricated during the immunosensor development were electrochemically characterized using EIS and CV techniques. EIS and CV analyses were performed in 5 mM $K_3Fe(CN)_6/K_4Fe(CN)_6$ containing 1 M KCl. The frequency range of EIS measurements was from 0.05 Hz to $5x10^4$ Hz. The potential of CV measurements was from -0.5 to 1 Vs. and the scan rate was 100 mV/s.

2.6 Measurement Procedures

All the fabrication steps of immunosensor were characterized by FTIR, Raman Spectroscopy, EIS, CV, SEM and AFM to confirm the successful fabrication of immunoelectrodes. During the fabrication process, the concentrations of PHP material and anti-IL-1α antibodies were optimized using a range from 0.025 mM to 0.1 mM, and a range from 0.4 ng/mL to 5 ng/mL, respectively. Other optimization parameters were antibody and antigen incubation durations. The response of the biosensor was tested after incubation from 30 min to 60 min. During the optimization experiments, the biosensor response was recorded electrochemically. In order to determine IL-1α antigen concentration, the prepared electrodes incubated in different concentrations of IL-1α solution. After incubation in antigen solution, the electrode surface was rinsed with ultrapure water to remove nonspecific adsorption of IL-1α antigen. The impedance response was measured as a function of the IL-1α concentration.

3. Results and Discussion

In this paper, an electrochemical biosensing approach for IL-1α antigen detection was proposed based on immunospecific interaction strategy coupled with EIS. As displayed in Scheme 1, the electrochemical biosensing mechanism was based on the specific interaction between anti-IL-1α antibody immobilized FTO electrode and IL-1α antigen. Anti-IL-1α antibodies were covalently immobilized on the surfaces of FTO/PHP, which provided to capture IL-1α antigen selectively.

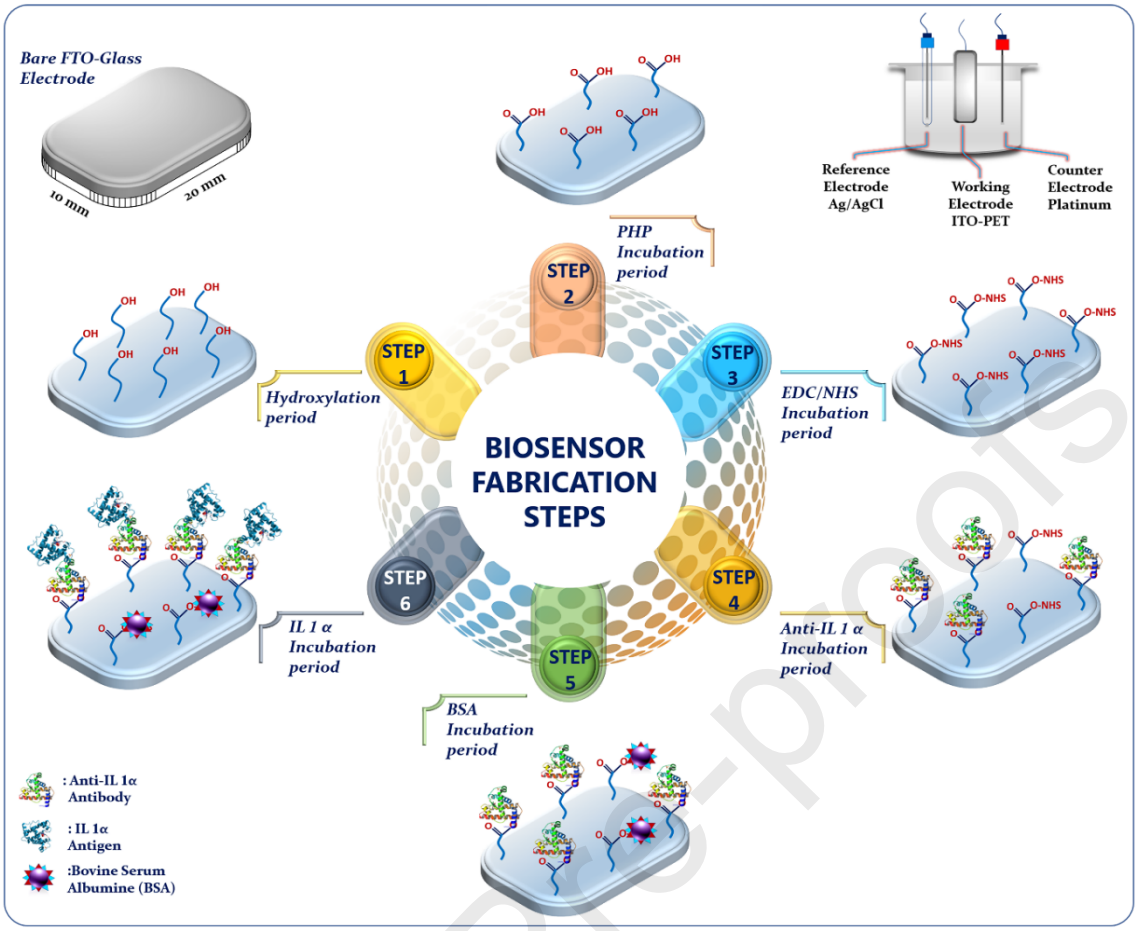

Scheme 1. Schematic representation for the detection of IL-1α using new PHP self-assembled FTO based electrochemical biosensor.

3.1 Chemical characterization modified FTO electrode surfaces

The electrode surface modification with interface material and biorecognition element immobilization onto the surface of FTO is a key step for the fabrication of the IL-1α biosensor proposed in this work, since the successful modification onto the FTO surface strongly affect the fabrication and performance of the biosensor. Therefore, the chemical characterizations of the modified electrode are important. FTIR and Raman spectroscopy methods were employed for chemical characterizations of modified FTO electrodes. At PHP modified FTO electrode, the characteristic peak of phosphonate bond (P-O-H), which formed between PHP and hydroxyl groups of FTO surface was monitored between 2550-2700 cm^{-1}[37, 38]. The PHP modified FTO electrode had the absorption peak at 1700 cm^{-1} due to carboxyl groups (C=O bonds) [39-41] (Fig. 1A). The similar peaks were observed in Raman spectra (Fig. 1C). The immobilization of anti-IL-1α antibodies changed the peaks observed in FTIR and Raman spectra. The peaks of amide bonds were seen at 1648 cm^{-1} and 1546 cm^{-1} in FTIR spectra (Fig. 1B). In Raman spectra, amid I, II and amid III regions are mostly observed between 1650-1680 cm^{-1}, 1440-1570 cm^{-1} and 1235-1300 cm^{-1} respectively [42]. As seen in Fig. 1D, the amid I, II and amide III peaks of this binding were seen at 1648 cm^{-1}, 1488 cm^{-1} and 1259 cm^{-1}, respectively.

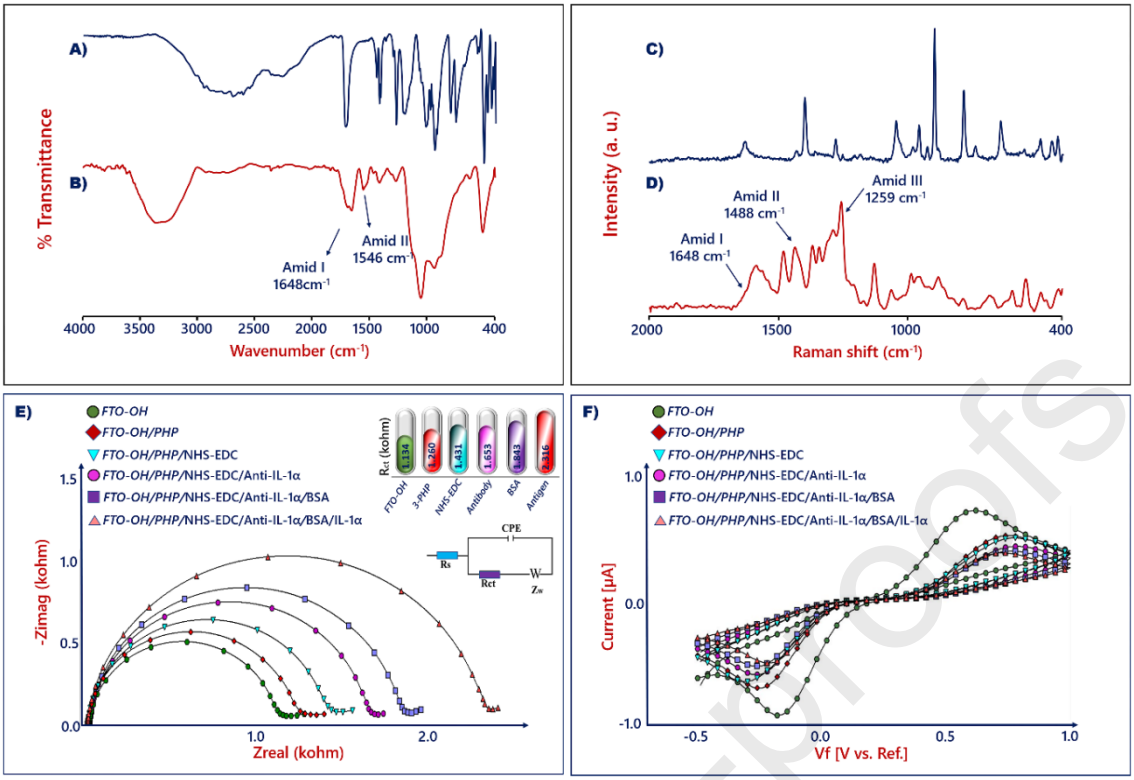

Figure 1. FTIR of FTO/PHP (A) and FTO/PHP/anti-IL-1α (B), and Raman spectra of FTO/PHP (C) and FTO/PHP/anti-IL-1α (D), Nyquist plots (E) and CVs (F) of stepwise assembly procedure. The electrochemical experiments were performed in 5.0 mM of $[Fe(CN)_6]^{3-/4-}$ containing 1 M of KCl (0.05 Hz–50 kHz); alternating potential: 5 mV, formal potential: 0 V.

3.2 Electrochemical characterization of the IL-1α biosensor

EIS is a successful method and provides valuable information on the variation in impedance behavior of the electrode [27, 43]. Because of this, EIS method was utilized to analyze the interface properties of FTO, FTO/PHP, FTO/PHP/anti-IL-1α, FTO/PHP/anti-IL-1α/BSA, FTO/PHP/anti-IL-1α/BSA/IL-1α. The Nyquist diagrams are displayed in Fig. 1E. The Randles equivalent circuit was employed for EIS measurements description (The fitted R_{ct} values of fabrication steps are shown in SI-Table 1A). Equivalent circuit contains the ohmic resistance of the electrolyte solution (R_Ω), the Warburg impedance (W) produced by ion diffusion from bulk electrolyte to the electrode interface, the constant phase element (CPE), the electron transfer resistance (R_{ct}) [44]. The diameter of the semicircle in Nyquist diagrams is associated to the R_{ct}. This resistance controls the electron-transfer kinetics of the redox couple at the electrode interface [27]. As seen in figure 1E, the hydroxylated FTO electrode had a small Nyquist plot with small R_{ct} value. This result illustrated that there was a little resistance against electron transfer at the FTO surface. After SAM formation on the FTO surface, a significant increase was observed in R_{ct} in comparison with the FTO/OH. This increase illustrated that the electron transfer process between the solution and PHP modified surface was prevented because of nonconductive property of PHP layer. After activation of carboxyl groups, an increase was observed in R_{ct} owing to

formation of a repellence between redox probe and negatively charged carboxyl groups. At the antibody immobilization step, an increase was seen in R_{ct}. This increase was attributed to the strong binding of anti-IL-1α antibodies on the PHP molecules. The EIS spectra of FTO/PHP/anti-BSA electrode showed a high R_{ct} than FTO/PHP/anti-IL-1α antibody electrode, because a nonconductive layer was constructed on the FTO surface. The free carboxyl ends were blocked by BSA and that prevented the electron transfer between modified electrode surface and electrolyte solution. Addition of IL-1α antigen onto FTO/PHP/anti-IL-1α/BSA surface increased the R_{ct} value and this behavior was attributed to the strong binding between anti-IL-1α antibodies and IL-1α antigens.

CV method was also utilized to follow the fabrication process of the proposed biosensor. CVs of the different modified surfaces in 5 mM $[Fe(CN)_6]^{3-/4-}$ are illustrated in Fig. 1F. A couple of redox peaks were observed after hydroxylation of FTO surface. The peak currents at the FTO/PHP decreased dramatically in comparison with FTO/OH surface. The reason of this decrease was that PHP was a nonconductive material and it prevented the electron transfer. The activation of carboxyl groups caused decreases in peak currents owing to the repellence of $[Fe(CN)_6]^{3-/4-}$ by the negatively charged carboxyl groups of PHP. The binding of anti-IL-1α antibodies on the PHP covered FTO surface caused inhibition of the electron transfer and hence, less electrical conductivity was formed. Therefore, the peak currents got smaller. The CV of FTO/PHP/anti-IL-1α/BSA showed decreases in peak currents as compared to FTO/PHP/anti-IL-1α bioelectrode, because the nonconductive property of BSA molecules and it prevented the electron transfer towards the electrode. The CV of FTO/PHP/anti-IL-1α/BSA/IL-1α bioelectrode showed decreases in peak currents as compared to the previous modification steps owing to the formation of immunocomplex which prevented the diffusion of the redox probe towards the electron surface. CV data were consistent with the EIS data, which further confirmed the successful fabrication of the biosensor.

3.3 Optimization of some factors during the biosensor fabrication

Some factors such as concentrations of PHP and anti-IL-1α antibodies, and incubation periods of anti-IL-1α antibodies and IL-1α antigen were optimized before the analytical characterization and investigation of immunosensor performance studies. First of all, the PHP concentration used for formation SAM was optimized. As shown in Fig. SI-1A, three different PHP concentrations were studied and the immunosensor had a maximum response when 0.05 mM PHP was utilized for fabrication of the biosensor. Therefore, 0.05 mM was selected the optimized concentration of PHP. The immunosensor response was affected by the concentrations of biorecognition molecule. Therefore, anti-IL-1α antibody concentrations from 0.4 to 5 ng/mL were tested and the obtained results were displayed in Fig. SI-1B. As seen in Fig. SI-1B, the best signal was obtained after incubation in phosphate buffer containing 2 ng/mL anti-IL-1α antibodies. Low level of anti-IL-1α antibody (0.4 ng/mL) induced a low signal and the increase in the concentration of anti-IL-1α antibody did not increase the biosensor signal. Also, incubation time of anti-IL-1α antibody and IL-1α antigen could affect the responses of the immunosensor. Fig. SI-1C illustrated the signals after 30 min, 45 min and 60 min incubations of

ITO/PHP/NHS-EDC electrode in phosphate buffer containing anti-IL-1α antibodies (2 ng/mL). The signals after 60 min incubation was higher than the other incubation times. Therefore, 60 min was chosen as the incubation duration necessary for binding of biorecognition element on the sensing interface. To optimize the IL-1α antigen incubation time, the suggested immunosensor was incubated with these antigens at various incubation durations (30 to 60 min). As seen in Fig. SI-1D, 45 min-incubation was adequate to reach a high immunosensor signal. Thus, 45 min was chosen as the optimal incubation duration between anti-IL-1α antibodies and IL-1α antigens. The optimized experimental conditions were summarized in Table 1A.

3.4 Morphological characterization of the fabricated IL-1α biosensor

SEM and AFM as useful tools for surface imaging were used in this work to get information about the modification process of the FTO based IL-1α biosensor. Fig. 2A and 2B illustrate the AFM and SEM images of PHP modified FTO surface. The SEM and AFM images of FTO/PHP electrode illustrated a homogenous structure due to organized SAM formation. The average roughness (R_a), which was a useful parameter for comparative analysis in AFM measurement, of this stage was 24 nm. The binding of anti-IL-1α antibodies on the PHP self-assembled FTO electrode changed the structure of the electrode and a uniform immobilization of the antibodies on the FTO electrode surface was seen (Figure 2C and 2D). From AFM measurements, the R_a of the FTO/PHP/anti-IL-1α (41 nm) was higher than PHP modified FTO electrode. The results confirmed the morphological change after the modification. After blockage of free carboxyl ends with BSA, a change was seen due to BSA immobilization (Figure 2E and 2F). As seen in Fig. 2F, a smooth surface was monitored, and the R_a of this stage was 27 nm. Fig. 2G and 2H showed the globular structures of IL-1α antigens found on the FTO surface. In Fig. 2H, IL-1α antigens were clearly seen on the electrode surface and from AFM measurements, the increase in R_a (41 nm) confirmed the successful specific interaction between anti-IL-1α antibodies and IL-1α antigens.

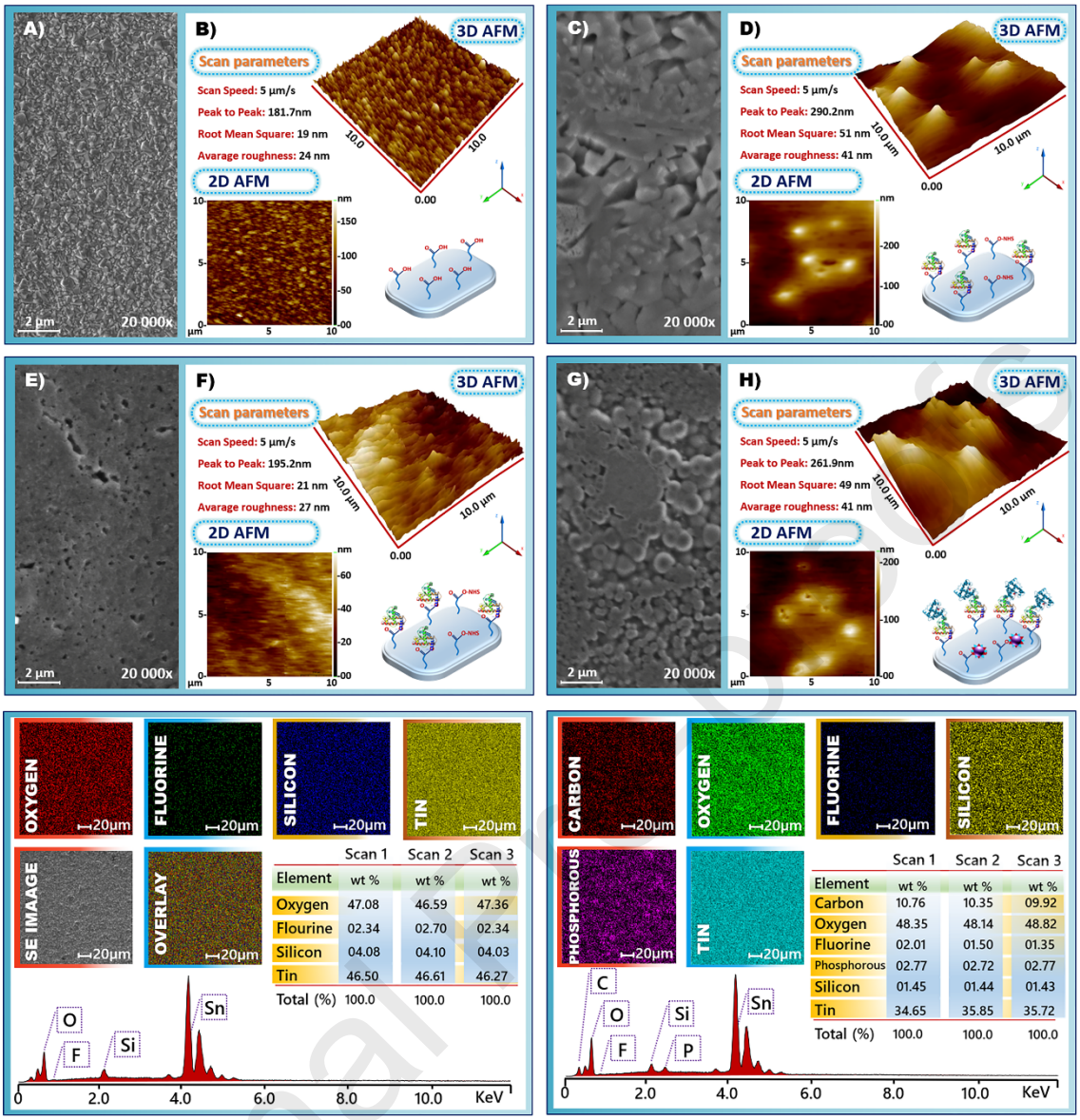

Figure 2. SEM and AFM images obtained after modification stages. SEM-EDX images of hydroxylated FTO (G) and PHP modified FTO (H).

Furthermore, the SEM-energy-dispersive X-ray (SEM-EDX) measurement was performed to monitor the PHP layer present on the FTO electrode. The SEM-EDX images of hydroxylated FTO electrode and PHP self-assembled FTO electrode surface are illustrated in Figure 2I and 2J, respectively. As displayed in Fig. 2I, hydroxylated FTO electrode had fluorine (F), tin (Sn) and oxygen (O) peaks. After self-assembling process of PHP on the FTO electrode, it had carbon (C), O, Sn, F, phosphorous (P) peaks on the FTO electrode surface (Fig. 2J). As observed in Fig. 2J, the ratios of P element in three different areas of the same electrodes were similar. Thus, the P peaks found on the FTO electrode indicated the successful coverage of PHP layer on the FTO surface.

3.5 Analytical performance of the immunosensor for IL-1α antigen detection

Under the optimal experiment conditions, the sensitivity and linear detection range of the biosensor for IL-1α detection were examined by impedimetric experiments. The EIS spectra and CVs of the FTO/PHP/anti-IL-1α/BSA were recorded after incubation with different levels of IL-1α antigen in the optimal conditions. Figure 3 displays EIS response of immunoelectrodes after interaction with IL-1α antigen concentration ranging from 0.02 to 2 ng/mL for 45 min. As the level of IL-1α antigen increased from 0.02 to 2 ng/mL, the diameter of Nyquist plot of the immunoelectrode increased due to the formation of more immunocomplex between anti-IL-1α antibody and IL-1α antigen that prevented the electron transfer (Fig. 3A) and the fitted R_{ct} values were shown in Table SI-1B. As shown in Fig. 3B, the peak currents after attachment of IL-1α antigen caused obvious decreases with increasing IL-1α antigen concentration. This decrease proved the successful attachment of IL-1α antigen on the immunosensor surface after reaction with the target IL-1α antigen. In sum, the increases in R_{ct} and the decreases in peak currents were originated from the rising immunocomplex amount on the electrode surface. From the Fig. 3C, it can be seen that the ΔR_{ct} had a good linear relationship with the concentration of IL-1α in the range from 0.02 to 2 ng/mL. The regression equation was ΔR_{ct}=1.594 [IL-1α] + 0.182 and the regression coefficient was 0.992. The limit of detection and limit of quantification were found as 6 fg/mL (*3s/m*) and 19 fg/mL (*10s/m*), respectively (s and m are the standard deviation of blank and the slope of calibration plot, respectively). In addition, sensitivity of the immunosensor was calculated as 6.90 kohm pg^{-1} mL cm^{-2}. The detection limit and linear detection range for IL-1α antigen of the suggested immunosensor were compared to other IL-1α detection techniques and better results were found (Table 1B). The high sensitivity of the suggested immunosensor could be originated from the specific interaction between anti-IL-1α antibody and IL-1α antigen, and the formation of well-ordered PHP SAMs. PHP provided a suitable matrix for successful binding of antibodies through strong covalent interaction by a well-known amide bond.

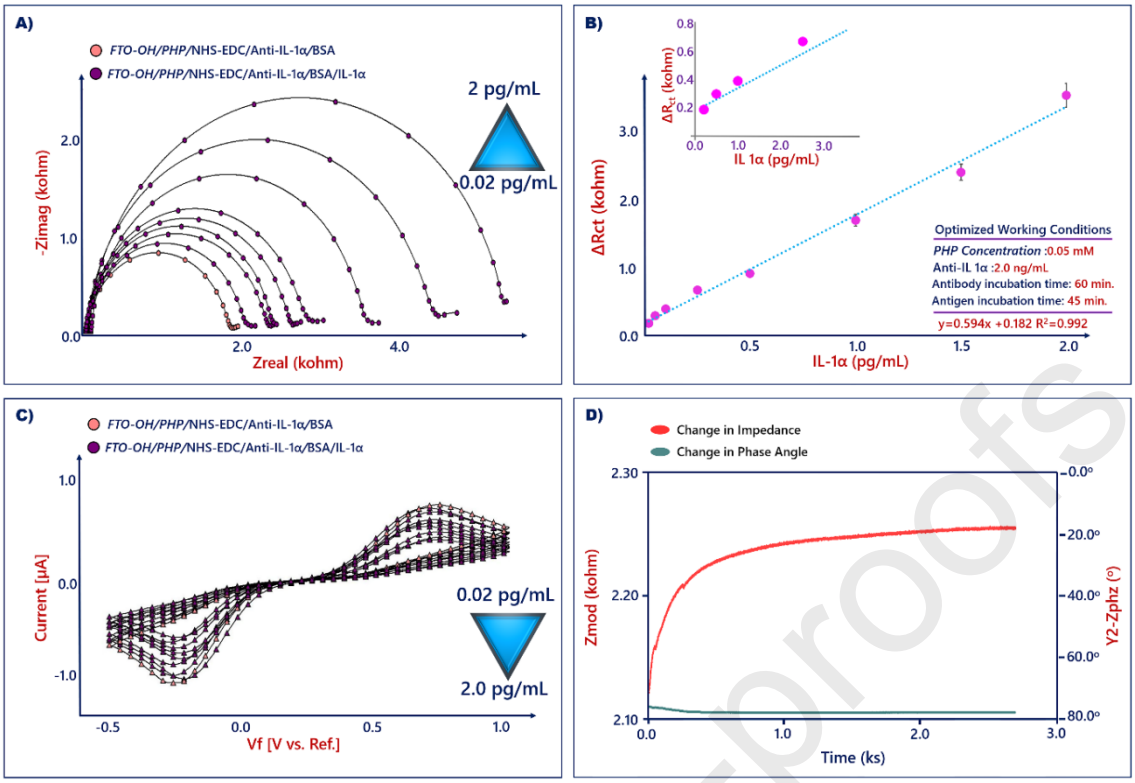

Figure 3. EIS spectra (A) and CVs of the fabricated biosensor with different levels of IL-1α antigen (0.02, 0.05, 0.1 ,0.25, 0.5, 1, 1.5, 2 pg/mL). Construction of calibration graphs between impedimetric signals and different levels of IL-1α antigen (C). Single frequency impedance analysis result (D).

Single frequency impedance (SFI) is an EIS method where a single frequency is employed as an excited signal instead of wide frequency range. This technique reduces the complexity in signal acquisition and processing, which makes it a proper and simple way for biomolecular sensing. In this technique, a constant frequency, which is identified with the help of Bode plot. Bode curve provides information about the kinetics at the electrode/solution interface for various several frequencies [45, 46]. The usage of this technique provides a great ability for a fast response, low cost, and low power analysis in the clinical and on field assays [47]. In this study, for the biomolecular sensing, 13 Hz was selected as an optimized frequency and an increase in impedance was observed resulting from antigen-antibody interactions (Figure 3D).

3.6 Repeatability, reproducibility, specificity, stability and reusability of the biosensor

The repeatability of the suggested immunosensor was examined by EIS measurements of 0.25 pg/mL IL-1α antigen solution. The relative standard deviation (RSD%) for twenty sequential measurements of IL-1α antigen was 4.85%, illustrating suitable repeatability of the biosensor (Figure 4A). To investigate the reproducibility of the immunosensor, 10 different immunosensors were fabricated independently and employed for IL-1α antigen measurement, and the RSD was 2.65%, revealed excellent reproducibility of the biosensor (Figure 4B).

The specificity of the suggested immunosensor was controlled by using several control species including TNF α, IL 8, IL 6 and IL 1β. A small impedimetric response was obtained in the presence of the control species and a high response in the presence of IL-1α illustrated the immunosensor specificity. The mixture of the above proteins did not affect the signal of IL-1α, this circumstance showed that the designed immunosensor was specific for IL-1α.

The reusability of the immunoelectrode was studied after regenerating it with acidic solution (HCl, 10 mM). After IL-1α antigen immobilization, the acidic regeneration process was performed to test the capture ability of antibodies present on the electrode surface to its antigens. After each regeneration process, the electrochemical responses of the immunosensor were recorded. After four successive regenerations, the proposed immunosensor retained 75.73% of its original response, indicating that it displayed reusability of 4 times (Figure 4C). Figure 4D depicts the long-term stability of the proposed immunosensor. The prepared bioelectrodes were stored at 4 °C for 8 weeks. The impedimetric response reduced %73.57 after 5 weeks storage, suggesting that the immunosensor was pretty stable when stored at 4 °C.

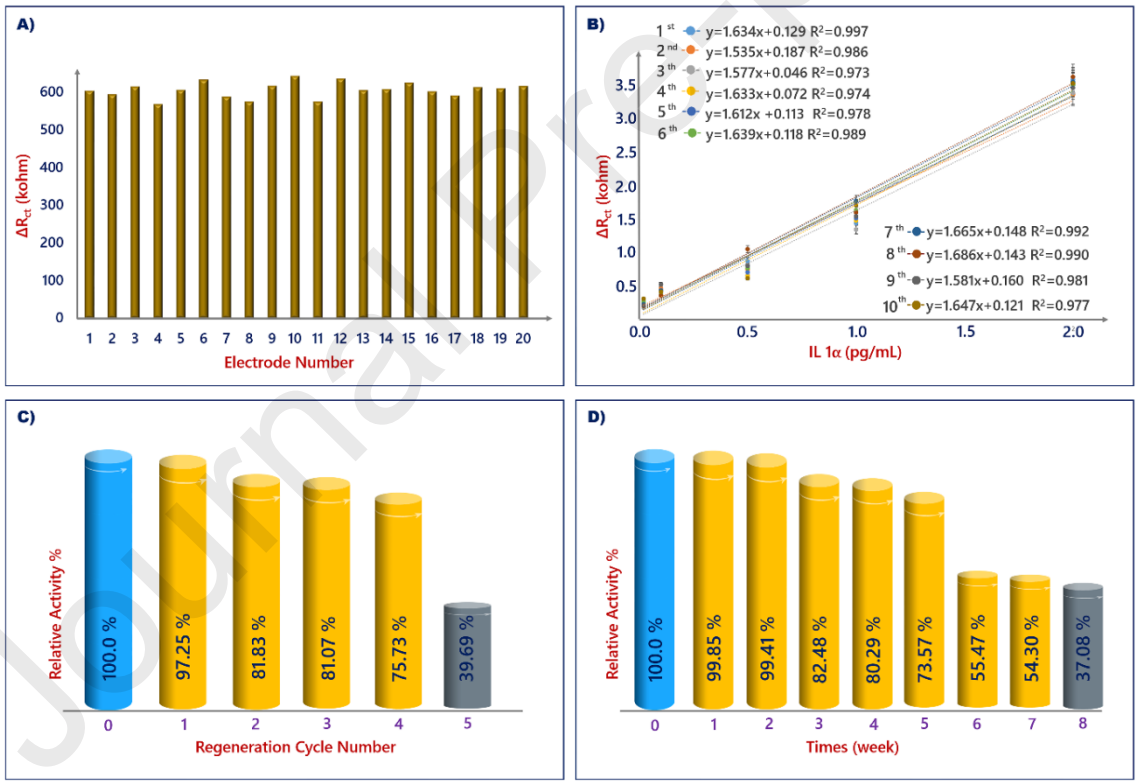

Figure 4. Repeatability (A), reproducibility (B), reusability (C) and storage-stability (D) results of the proposed immunosensor.

3.7 Analysis of clinical serum samples

The applicability of the immunosensor for human biological sample analyses is important [48-50]. To illustrate the ability of the proposed immunosensor for the determination of IL-1α antigen in real

samples, human serum samples and saliva samples were analyzed. Before the analysis by the designed biosensor, serum and saliva samples were diluted 200 and 20-fold, respectively. Moreover, IL-1α antigens (at known concentrations) were added into the serum and saliva samples to determine the accuracy of the proposed immunosensor. The recovery values of saliva (100.36-103.04%) and serum (99.53-103.58%) samples were acceptable, indicating that our immunosensor could potentially detect the IL-1α n human serum samples (Table 1C and 1D).

Table 1. Optimized experimental conditions (A), comparison of different methods for detection of IL-1α (B), the analysis results of human serum (C) and saliva (D) samples.

A) Variable	**Tested**	**Selected**
PHP concentration	0.025 mM, 0.05 mM, 0.1 mM	0.05 mM
Anti-IL-1α concentration	0.40 ng/mL, 2.0 ng/mL, 5.0 ng/mL	2.0 ng/mL
Anti-IL-1α incubation time	30 min, 45 min, 60 min	60 minutes
IL-1α antigen incubation time	30 min, 45 min, 60 min	45 minutes

B) Biosensing System	**Measurement principle**	**Linear Range**	**Detection limit**	**References**
Xerogels with integrated emission sites	Optic	-	2 pg/mL	[16]
Quantum dots modified electrochemical immunoassay	Amperometric	0.5-50 ng/mL	0.3 ng/mL	[18]
Carboxymethyl dextran modified cuvette surface	Optic	100-1600 nM	100 nM	[17]
PHP modified ITO electrode	Impedimetric	0.02-2 pg/mL	6 fg/mL	This study
ELISA kit	Colorimetric	31.2-1000 pg/mL	10 pg/mL	Abcam
ELISA kit	Colorimetric	1.6-100 pg/mL	1.1 pg/mL	Thermo-fischer
ELISA kit	Colorimetric	4.7-300 pg/mL	0.5 pg/mL	Mybiosource
ELISA kit	Colorimetric	3.91-250 pg/mL	2.35 pg/mL	Elabscience

C) Serum	**Found by biosensor (pg/mL)**	**Added IL-1α antigen (pg/mL)**	***SD and *CV (%)**	**Total found by biosensor**	***SD and *CV (%)**	**Recovery (%)**	**Relative difference (%)**
1	0.39	0.5	0.02, 3.89	0.89	0.02, 2.59	100.33	0.33
1	0.41	0.5		0.92		101.57	1.57
2	0.46	0.5	0.02, 3.50	0.95	0.02, 1.84	99.59	-0.41
2	0.48	0.5		0.98		99.79	-0.21
(3	0.32	0.5	0.01, 4.47	0.85	0.01, 1.06	103.58	3.58
3	0.34	0.5		0.83		99.53	-0.47
4	0.45	0.5	0.03, 5.73	0.96	0.02, 2.28	100.24	0.24
4	0.49	0.5		0.99		99.54	-0.46
5	0.66	0.5	0.03, 4.77	1.16	0.03, 2.89	99.55	-0.45
5	0.71	0.5		1.21		99.73	-0.27

*SD: Standard Deviation, *CV: Coefficient Variation.

D) Saliva	**Found by biosensor (pg/mL)**	**Added IL-1α antigen (pg/mL)**	***SD and *CV (%)**	**Total found by biosensor**	***SD and *CV (%)**	**Recovery (%)**	**Relative difference (%)**
1	1.10	0.5	0.04, 3.19	1.65	0.01, 0.67	103.04	3.04
1	1.15	0.5		1.67		100.82	0.82
2	0.67	0.5	0.04, 6.33	1.18	0.05, 4.39	100.52	0.52
2	0.73	0.5		1.25		101.51	1.51
3	1.00	0.5	0.03, 2.74	1.53	0.03, 1.72	101.78	1.78
3	1.04	0.5		1.57		101.62	1.62
4	0.67	0.5	0.02, 2.90	1.18	0.02, 1.68	100.36	0.36
4	0.70	0.5		1.21		100.35	0.35
5	0.32	0.5	0.01, 4.10	0.82	0.02, 1.92	100.67	0.67
5	0.33	0.5		0.84		101.11	1.11

*SD: Standard Deviation, *CV: Coefficient Variation.

4. Conclusion

In summary, a facile electrochemical immunosensor based on PHP was first developed for sensitive IL-1α detection. The suggested immunosensor was constructed by binding of anti-IL-1α antibodies on the PHP self-assembled FTO surface. The usage of PHP provided well-ordered SAMs and a biocompatible electrode surface for attachment of anti-IL-1α antibodies. The impedimetric signals of the immunosensor was increased by increasing IL-1α level and R_{ct} positively correlated with IL-1α level. The interfacial R_{ct} difference was probed via EIS and Randles equivalent circuit. The designed immunosensor could detect IL-1α biomarker in a range from 0.02 to 2 pg/mL with a limit of detection of 6 fg/mL, which was lower than other studies found in literature. The designed self-assembly strategy of this impedimetric immunosensor was successfully applied to the analysis of the human serum and saliva samples, and satisfactory recovery results were obtained. The developed immunosensor could be a very attractive tool to quantify the IL-1α antigen level owing to its sensitivity, stability, specificity and cost effectiveness. Consequently, it is believed that this immunosensor could be promisingly used for early diagnosis of cancer.

References

[1] R.S. Malon, S. Sadir, M. Balakrishnan, E.P. Córcoles, Saliva-based biosensors: noninvasive monitoring tool for clinical diagnostics, BioMed Res. Int, 2014 (2014).
[2] S. Abdul Rehman, Z. Khurshid, F. Hussain Niazi, M. Naseem, H. Al Waddani, H.A. Sahibzada, R. Sannam Khan, Role of salivary biomarkers in detection of cardiovascular diseases (CVD), Proteomes, 5 (2017) 21.
[3] H. Jasim, A. Carlsson, B. Hedenberg-Magnusson, B. Ghafouri, M. Ernberg, Saliva as a medium to detect and measure biomarkers related to pain, Sci. Rep. 8 (2018) 1-9.
[4] I.T. Gug, M. Tertis, O. Hosu, C. Cristea, Salivary biomarkers detection: Analytical and immunological methods overview, TrAC, Trends Anal. Chem. 113 (2019) 301-316.
[5] B.-Y. Wu, J. Li, J.-D. Huang, Y.-Y. Wang, H.-J. Yin, K.-J. Chen, Q. Chen, Real time kinetic analysis of the interaction between interleukin-1α and soluble interleukin-1 receptor I using a resonant mirror biosensor, Anal. Chim. Acta, 557 (2006) 106-110.
[6] K. Snoussi, A.D. Strosberg, N. Bouaouina, S. Ben Ahmed, L. Chouchane, Genetic variation in pro-inflammatory cytokines (interleukin-1beta, interleukin-1alpha and interleukin-6) associated with the aggressive forms, survival, and relapse prediction of breast carcinoma, Eur. Cytokine Network, 16 (2005) 253-260.
[7] T. Sultana, K. Svechnikov, G.n. Weber, O. Söder, Molecular cloning and expression of a functionally different alternative splice variant of prointerleukin-1α from the rat testis, Endocrinology, 141 (2000) 4413-4418.
[8] E. Dursun, D. Gezen-Ak, H. Hanağası, B. Bilgiç, E. Lohmann, S. Ertan, İ.L. Atasoy, M. Alaylıoğlu, Ö.S. Araz, B. Önal, The interleukin 1 alpha, interleukin 1 beta, interleukin 6 and alpha-2-macroglobulin serum levels in patients with early or late onset Alzheimer's disease, mild cognitive impairment or Parkinson's disease, J. Neuroimmunol. 283 (2015) 50-57.
[9] J.A. Royall, R.L. Berkow, J.S. Beckman, M.K. Cunningham, S. Matalon, B.A. Freeman, Tumor necrosis factor and interleukin 1 alpha increase vascular endothelial permeability, American Journal of Physiology-Lung Cellular and Molecular Physiology, 257 (1989) L399-L410.
[10] Y.R. Chianeh, K. Prabhu, Biochemical markers in saliva of patients with oral squamous cell carcinoma, Asian Pac. J. Trop. Dis., 4 (2014) S33-S40.
[11] R. Mishra, Biomarkers of oral premalignant epithelial lesions for clinical application, Oral Oncol. 48 (2012) 578-584.
[12] H. Polanska, M. Raudenska, J. Gumulec, M. Sztalmachova, V. Adam, R. Kizek, M. Masarik, Clinical significance of head and neck squamous cell cancer biomarkers, Oral Oncol. 50 (2014) 168-177.
[13] N. Russo, E. Bellile, C.A. Murdoch-Kinch, M. Liu, A. Eisbruch, G.T. Wolf, N.J. D'silva, Cytokines in saliva increase in head and neck cancer patients after treatment, Oral surgery, oral medicine, oral pathology and oral radiology, 122 (2016) 483-490. e481.
[14] A. Korostoff, L. Reder, R. Masood, U.K. Sinha, The role of salivary cytokine biomarkers in tongue cancer invasion and mortality, Oral Oncol. 47 (2011) 282-287.
[15] A.-W.R. Hamad, S.M. Gaphor, M.T. Shawagfeh, N.G. Al-Talabani, Study of serum and salivary levels of proinflammatory cytokines, potential biomarkers in the diagnosis of oral squamous cell carcinoma, Acad. J. Cancer, 4 (2011) 47-55.
[16] Z. Tao, E.C. Tehan, R.M. Bukowski, Y. Tang, E.L. Shughart, W.G. Holthoff, A.N. Cartwright, A.H. Titus, F.V. Bright, Templated xerogels as platforms for biomolecule-less biomolecule sensors, Anal. Chim. Acta, 564 (2006) 59-65.
[17] B.-y. Wu, Y.-y. Wang, J. Li, Z. Song, J.-d. Huang, X.-s. Wang, Q. Chen, An optical biosensor for kinetic analysis of soluble Interleukin-1 receptor I binding to immobilized Interleukin-1α, Talanta, 70 (2006) 485-488.
[18] H. Wu, G. Liu, J. Wang, Y. Lin, Quantum-dots based electrochemical immunoassay of interleukin-1α, Electrochem. Commun. 9 (2007) 1573-1577.

[19] F. Lamberti, S. Agnoli, L. Brigo, G. Granozzi, M. Giomo, N. Elvassore, Surface functionalization of fluorine-doped tin oxide samples through electrochemical grafting, ACS Appl. Mater. Interfaces, 5 (2013) 12887-12894.
[20] Y. Liu, K. Peters, B. Mandlmeier, A. Müller, K. Fominykh, J. Rathousky, C. Scheu, D. Fattakhova-Rohlfing, Macroporous indium tin oxide electrode layers as conducting substrates for immobilization of bulky electroactive guests, Electrochim. Acta, 140 (2014) 108-115.
[21] M. Noroozifar, M. Khorasani-Motlagh, H.H. Nadiki, M.S. Hadavi, M.M. Foroughi, Modified fluorine-doped tin oxide electrode with inorganic ruthenium red dye-multiwalled carbon nanotubes for simultaneous determination of a dopamine, uric acid, and tryptophan, Sens. Actuators, B, 204 (2014) 333-341.
[22] S.A. Ansari, A. Ahmed, F.K. Ferdousi, M.A. Salam, A. Shaikh, H.R. Barai, N.S. Lopa, M.M. Rahman, Conducting poly (aniline blue)-gold nanoparticles composite modified fluorine-doped tin oxide electrode for sensitive and non-enzymatic electrochemical detection of glucose, Journal of Electroanal. Chem. 850 (2019) 113394.
[23] K.-T. Lee, D.-M. Liu, Y.-Y. Liang, N. Matsushita, T. Ikoma, S.-Y. Lu, Porous fluorine-doped tin oxide as a promising substrate for electrochemical biosensors—demonstration in hydrogen peroxide sensing, . J. Mater. Chem. B, 2 (2014) 7779-7784.
[24] S. Panky, K. Thandavan, D. Sivalingam, S. Sethuraman, U.M. Krishnan, B.G. Jeyaprakash, J.B.B. Rayappan, Lipase immobilized on nanostructured cerium oxide thin film coated on transparent conducting oxide electrode for butyrin sensing, Mater. Chem. Phys. 137 (2013) 892-897.
[25] A.-J. Wang, X.-Y. Zhu, Y. Chen, X. Luo, Y. Xue, J.-J. Feng, Ultrasensitive label-free electrochemical immunoassay of carbohydrate antigen 15-3 using dendritic Au@ Pt nanocrystals/ferrocene-grafted-chitosan for efficient signal amplification, Sens. Actuators, B, 292 (2019) 164-170.
[26] A.-J. Wang, X.-Y. Zhu, Y. Chen, P.-X. Yuan, X. Luo, J.-J. Feng, A label-free electrochemical immunosensor based on rhombic dodecahedral Cu3Pt nanoframes with advanced oxygen reduction performance for highly sensitive alpha-fetoprotein detection, Sens. Actuators, B, 288 (2019) 721-727.
[27] H. Bagheri, R. Talemi, A. Afkhami, Gold nanoparticles deposited on fluorine-doped tin oxide surface as an effective platform for fabricating a highly sensitive and specific digoxin aptasensor, RSC Adv. 5 (2015) 58491-58498.
[28] N. Prabhakar, H. Thakur, A. Bharti, N. Kaur, Chitosan-iron oxide nanocomposite based electrochemical aptasensor for determination of malathion, Analytica Chim. Acta, 939 (2016) 108-116.
[29] M.M. Khan, S.A. Ansari, J. Lee, M.H. Cho, Novel Ag@ TiO2 nanocomposite synthesized by electrochemically active biofilm for nonenzymatic hydrogen peroxide sensor, Mater. Sci. Eng.,C, 33 (2013) 4692-4699.
[30] N. Chauhan, S. Chawla, C. Pundir, U. Jain, An electrochemical sensor for detection of neurotransmitter-acetylcholine using metal nanoparticles, 2D material and conducting polymer modified electrode, Biosens. Bioelectron., 89 (2017) 377-383.
[31] S.A. Ansari, Z. Khatoon, N. Parveen, H. Fouad, A. Kulkarni, A. Umar, Z. Ansari, S. Ansari, Polyaniline-functionalized TiO2 nanoparticles as a suitable matrix for hydroquinone sensor, Science of Advanced Materials, 9 (2017) 2032-2038.
[32] R.V. Jagadeesh, V. Lakshminarayanan, Adsorption kinetics of phosphonic acids and proteins on functionalized Indium tin oxide surfaces using electrochemical impedance spectroscopy, Electrochim. Acta, 197 (2016) 1-9.
[33] I. Gouzman, M. Dubey, M.D. Carolus, J. Schwartz, S.L. Bernasek, Monolayer vs. multilayer self-assembled alkylphosphonate films: X-ray photoelectron spectroscopy studies, Surf. Sci. 600 (2006) 773-781.
[34] K. Jo, H.-Z. Yu, H. Yang, Formation kinetics and stability of phosphonate self-assembled monolayers on indium–tin oxide, Electrochim. Acta, 56 (2011) 4828-4833.
[35] B. Zhang, T. Kong, W. Xu, R. Su, Y. Gao, G. Cheng, Surface functionalization of zinc oxide by carboxyalkylphosphonic acid self-assembled monolayers, Langmuir, 26 (2010) 4514-4522.
[36] M. Dubey, T. Weidner, L.J. Gamble, D.G. Castner, Structure and order of phosphonic acid-based self-assembled monolayers on Si (100), Langmuir, 26 (2010) 14747-14754.

[37] L. Daasch, D. Smith, Infrared spectra of phosphorus compounds, Anal. Chem. 23 (1951) 853-868.
[38] R. Luschtinetz, G. Seifert, E. Jaehne, H.J.P. Adler, Infrared spectra of alkylphosphonic acid bound to aluminium surfaces, Macromolecular symposia, Wiley Online Library, 2007, pp. 248-253.
[39] K. Khaldi, S. Sam, A. Gouget-Laemmel, C. Henry de Villeneuve, A. Moraillon, F. Ozanam, J. Yang, A. Kermad, N. Ghellai, N. Gabouze, Active acetylcholinesterase immobilization on a functionalized silicon surface, Langmuir, 31 (2015) 8421-8428.
[40] M. Aydın, E.B. Aydın, M.K. Sezgintürk, A disposable immunosensor using ITO based electrode modified by a star-shaped polymer for analysis of tumor suppressor protein p53 in human serum, Biosens. Bioelectron. 107 (2018) 1-9.
[41] E.B. Aydın, M. Aydın, M.K. Sezgintürk, A highly sensitive immunosensor based on ITO thin films covered by a new semi-conductive conjugated polymer for the determination of TNFα in human saliva and serum samples, Biosens. Bioelectron. 97 (2017) 169-176.
[42] M. Aydın, A sensitive and selective approach for detection of IL 1α cancer biomarker using disposable ITO electrode modified with epoxy-substituted polythiophene polymer, Biosens. Bioelectron. 144 (2019) 111675.
[43] Y. Chen, L.-P. Mei, J.-J. Feng, P.-X. Yuan, X. Luo, A.-J. Wang, Simple one-pot aqueous synthesis of 3D superstructured PtCoCuPd alloyed tripods with hierarchical branches for ultrasensitive immunoassay of cardiac troponin I, Biosens. Bioelectron.145 (2019) 111638.
[44] H.P. Nascimento, M.D. Oliveira, C.P. de Melo, G.J. Silva, M.T. Cordeiro, C.A. Andrade, An impedimetric biosensor for detection of dengue serotype at picomolar concentration based on gold nanoparticles-polyaniline hybrid composites, Colloids Surf., B 86 (2011) 414-419.
[45] M. Aydın, E.B. Aydın, M.K. Sezgintürk, A Highly Selective Poly (thiophene)-graft-Poly (methacrylamide) Polymer Modified ITO Electrode for Neuron Specific Enolase Detection in Human Serum, Macromol. Biosci. 19 (2019) 1900109.
[46] M. Aydın, E.B. Aydın, M.K. Sezgintürk, Electrochemical immunosensor for CDH22 biomarker based on benzaldehyde substituted poly (phosphazene) modified disposable ITO electrode: A new fabrication strategy for biosensors, Biosens. Bioelectron. 126 (2019) 230-239.
[47] S. Singal, R.K. Kotnala, Single frequency impedance analysis on reduced graphene oxide screen-printed electrode for biomolecular detection, . Appl. Biochem. Biotechnol. 183 (2017) 672-683.
[48] Y. Chen, X.-Y. Ge, S.-Y. Cen, A.-J. Wang, X. Luo, J.-J. Feng, Ultrasensitive dual-signal ratiometric electrochemical aptasensor for neuron-specific enolase based on Au nanoparticles@ Pd nanoclusters-poly (bismarck brown Y) and dendritic AuPt nanoassemblies, Sens. Actuators, B, (2020) 127931.
[49] E.B. Aydın, M. Aydın, M.K. Sezgintürk, Construction of succinimide group substituted polythiophene polymer functionalized sensing platform for ultrasensitive detection of KLK 4 cancer biomarker, Sens. Actuators, B, 325 (2020) 128788.
[50] E.B. Aydın, M. Aydın, M.K. Sezgintürk, A novel electrochemical immunosensor based on acetylene black/epoxy-substituted-polypyrrole polymer composite for the highly sensitive and selective detection of interleukin 6, Talanta, 222 121596.

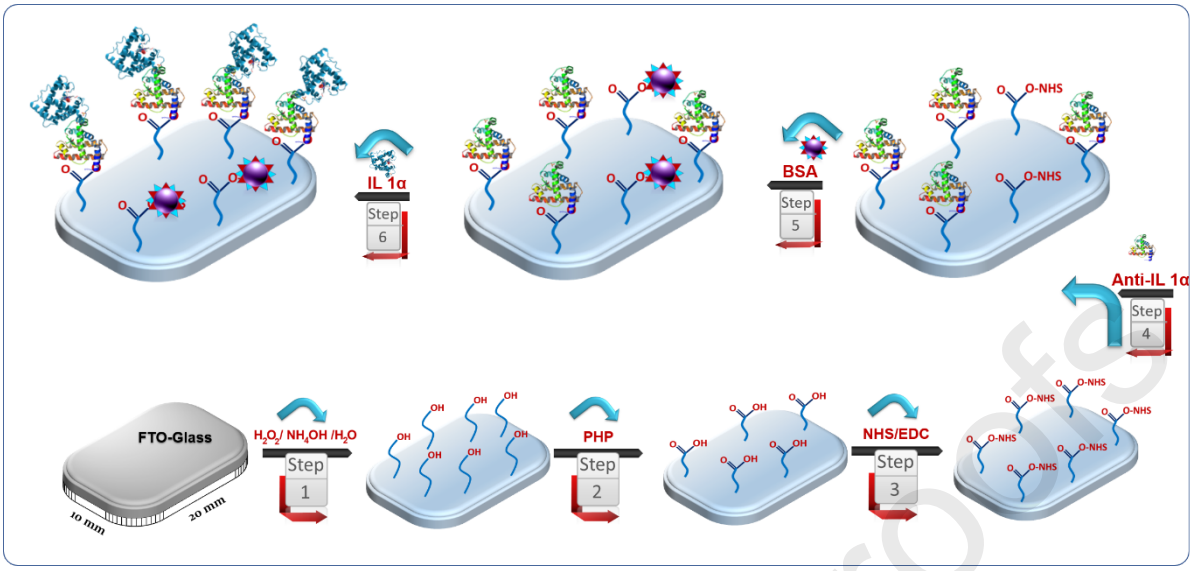

Highlights

- An EIS immunosensor based on carboxyalkylphosphonic acid covered FTO electrode was developed for the determination of IL-1α.
- The prepared immunosensor was characterized by several electrochemical and morphological techniques.
- The prepared immunosensor showed high stability, good repeatability, excellent reproducibility and reusability.
- The proposed biosensor could detect the IL-1α in clinical samples.

Table 1. Optimized experimental conditions (A), comparison of different methods for detection of IL-1α (B), the analysis results of human serum (C) and saliva (D) samples.

A) Variable	**Tested**	**Selected**
PHP concentration	0.025 mM, 0.05 mM, 0.1 mM	0.05 mM
Anti-IL-1α concentration	0.40 ng/mL, 2.0 ng/mL, 5.0 ng/mL	2.0 ng/mL
Anti-IL-1α incubation time	30 min, 45 min, 60 min	60 minutes
IL-1α antigen incubation time	30 min, 45 min, 60 min	45 minutes

B) Biosensing System	**Measurement principle**	**Linear Range**	**Detection limit**	**References**
Xerogels with integrated emission sites	Optic	-	2 pg/mL	[16]
Quantum dots modified electrochemical immunoassay	Amperometric	0.5-50 ng/mL	0.3 ng/mL	[18]
Carboxymethyl dextran modified cuvette surface	Optic	100-1600 nM	100 nM	[17]
PHP modified FTO electrode	Impedimetric	0.02-2 pg/mL	6 fg/mL	This study
ELISA kit	Colorimetric	31.2-1000 pg/mL	10 pg/mL	Abcam
ELISA kit	Colorimetric	1.6-100 pg/mL	1.1 pg/mL	Thermo-fischer
ELISA kit	Colorimetric	4.7-300 pg/mL	0.5 pg/mL	Mybiosource
ELISA kit	Colorimetric	3.91-250 pg/mL	2.35 pg/mL	Elabscience

C) Serum	**Found by biosensor (pg/mL)**	**Added IL-1α antigen (pg/mL)**	***SD and *CV (%)**	**Total found by biosensor**	***SD and *CV (%)**	**Recovery (%)**	**Relative difference (%)**
1	0.39	0.5	0.02, 3.89	0.89	0.02, 2.59	100.33	0.33
1	0.41	0.5		0.92		101.57	1.57
2	0.46	0.5	0.02, 3.50	0.95	0.02, 1.84	99.59	-0.41
2	0.48	0.5		0.98		99.79	-0.21
(3	0.32	0.5	0.01, 4.47	0.85	0.01, 1.06	103.58	3.58
3	0.34	0.5		0.83		99.53	-0.47
4	0.45	0.5	0.03, 5.73	0.96	0.02, 2.28	100.24	0.24
4	0.49	0.5		0.99		99.54	-0.46
5	0.66	0.5	0.03, 4.77	1.16	0.03, 2.89	99.55	-0.45
5	0.71	0.5		1.21		99.73	-0.27

*SD: Standard Deviation, *CV: Coefficient Variation.

D) Saliva	**Found by biosensor (pg/mL)**	**Added IL-1α antigen (pg/mL)**	***SD and *CV (%)**	**Total found by biosensor**	***SD and *CV (%)**	**Recovery (%)**	**Relative difference (%)**
1	1.10	0.5	0.04, 3.19	1.65	0.01, 0.67	103.04	3.04
1	1.15	0.5		1.67		100.82	0.82
2	0.67	0.5	0.04, 6.33	1.18	0.05, 4.39	100.52	0.52
2	0.73	0.5		1.25		101.51	1.51
3	1.00	0.5	0.03, 2.74	1.53	0.03, 1.72	101.78	1.78
3	1.04	0.5		1.57		101.62	1.62
4	0.67	0.5	0.02, 2.90	1.18	0.02, 1.68	100.36	0.36
4	0.70	0.5		1.21		100.35	0.35
5	0.32	0.5	0.01, 4.10	0.82	0.02, 1.92	100.67	0.67

5	0.33	0.5	0.84	101.11	1.11

*SD: Standard Deviation, *CV: Coefficient Variation.

Declaration of interests

☒ The authors declare that they have no known competing financial interests or personal relationships that could have appeared to influence the work reported in this paper.

☐The authors declare the following financial interests/personal relationships which may be considered as potential competing interests: